Analytical and Bioanalytical Chemistry (2023) 415:2193–2207
https://doi.org/10.1007/s00216-023-04625-7

RESEARCH PAPER

Separation of mass spectra of hydrogen–deuterium exchanged ions obtained by electrospray of solutions of biopolymers with unknown primary structure

Valery Raznikov[1] · Marina Raznikova[2] · Ilia Sulimenkov[1] · Vladislav Zelenov[1]

Received: 10 January 2023 / Accepted: 21 February 2023 / Published online: 21 March 2023

Abstract
The work is dedicated to further development of our described method for analyzing mass spectra of biomolecules acquired as a result of hydrogen–deuterium exchange reactions (HDXs). The modified method consists of separating HDX distributions via their approximations by a minimum number of components corresponding to independent H/D substitutions and independent charge carrier retentions in different spatial isoforms or conformations of biomolecules with unknown primary structures. In this case, neither the natural isotopic distribution nor the exact number of active sites involved in HDXs and H^+ or D^+ attachments can be determined in advance. Original H/D electrospray mass spectra of an apamin solution were taken from our previous work. In that work, taking into account the natural isotopic distribution of apamin molecules, three main conformations of apamin ions were found as a result of separating the H/D mass spectra of the apamin solution for the gas flow with the addition of about 10% ND_3 molecules. Using the proposed modified method that does not require knowledge of the primary structure of the biomolecules gave similar results with slight deviations of calculated HDX distributions of the apamin ions from those obtained earlier. The maximum difference between mean values of the calculated HDX distributions for ions of the same charge in both cases does not exceed a few percent. In addition, HDX mass spectra of the apamin complex with an adduct of unknown structure were processed. Such analysis gave also three main fractions of ions with relatively large contributions when ND_3 was injected into a radio-frequency quadrupole. In the absence of ND_3 flow, the results of calculations for apamin and its complex were close to each other too. The formation of the apamin complex most probably in solution was confirmed by performed calculations.

Keywords Electrospray mass spectrometry · H/D exchange · Proton and deuteron retention probabilities · Central limit theorem

Introduction

The determination of changes in the native structure of proteins in solutions may be important for solving many problems including early diagnosis of Alzheimer's, Parkinson's, and Huntington's diseases. It is believed that the folded globule partial opening may indicate the ability of these proteins to form fibril-like structures, which leads in turn to the development of such diseases. Therefore, achieving high sensitivity and information density in a relatively short analysis time is in this case not only of theoretical interest. Mass spectrometry in combination with other modern methods of separation of biopolymer mixtures ensures maximum sensitivity and reliability of identification, in particular of known proteins, or allows us at least a partial establishment of their primary structure when such proteins are not in the relevant databases. Mass-spectrometric data obtained by electrospray ionization of solutions gives an opportunity, as a rule, to distinguish between folded and denatured forms of the protein based on the width of the charge distributions of its multicharged ions. A more detailed analysis of these

✉ Valery Raznikov
raznikov@hotmail.com

✉ Marina Raznikova
raznikova.mari@yandex.ru

[1] Chernogolovka Branch of the N.N. Semenov Federal Research Center for Chemical Physics, Russian Academy of Sciences, Chernogolovka, Moscow 142432, Russia

[2] Federal Research Center of Problems of Chemical Physics and Medicinal Chemistry, Russian Academy of Sciences, Chernogolovka, Moscow 142432, Russia

distributions, obtained, for example, by H/D exchange, could open up the possibility of detecting relatively small changes in the spatial structure of the protein molecules in solution.

Since the 1950s, the hydrogen–deuterium exchange (HDX) is widely used in structural and conformational studies of biomolecules. The transition to mass spectrometric measurements (HDX-MS) happened in the 1990s, including the ionization of biomolecule solutions by electrospray. A very informative review of this and somewhat later period is given in [1]. Currently, it is a growing highly diversified area. The first international conference on hydrogen exchange mass spectrometry was held in 2017 (Gothenburg, Sweden). A number of participants of this conference (more than 40 people) presented their recommendations for conducting and interpreting classical HDX-MS measurements [2] for proteins and their complexes. The application areas of the HDX-MS method and the stages of sample preparation and measurements were structurally described in this work. Among them, the HDX quench, enzymatic hydrolysis, UHPLC separation of the resulting peptides, and their mass analysis with the interpretation of the data obtained were considered. To obtain quantitative conclusions about the degree of HDX in the isolated peptides, it is assumed that the entire sequence of described measurements is performed including the initial absence of HDX of the original biomolecules or when the contact time of these biomolecules with D_2O has being changed.

Actually, this approach was the further evolution of a technique originally developed and widely used earlier to probe $^1H/^3H$ exchange for the protein investigation. The group headed by D.L. Smith was the first to realize the transition from ^3H to ^2H in this approach and actually implemented about 30 years ago the steps close to those just described [3].

This method seems to be very informative for the proteins with a single or close several spatial structural forms in investigated samples. Otherwise, it may be difficult to assign peptides after hydrolysis to specific protein spatial isoforms.

A detailed review of various aspects of HDX-MS measurements including those that differ from classical approaches was provided in [4]. In particular, the review is of value for studying the conformational dynamics of biomolecules, as well as for obtaining essential information about the structure of individual compounds and the composition of complex natural mixtures. A detailed overview of the pharmaceutical applications of HDX-MS measurements is presented in [5].

The reactions of hydrogen–deuterium exchange in solution are likely to be most important for obtaining the information about a "natural" structure of biopolymers. However, for a usual electrospray ion source, the processes of H/D substitution of biomolecules in the gas phase are expected to be inevitable. Thus, not only theoretical interest in this case is represented by investigation of such processes [6, 7]. Kinetic HDX measurements can be used to characterize various exchangeable hydrogen atoms of a biomolecule [8]. However, this characterization is only possible for hydrogen atoms that differ significantly in the ability of H/D substitution. In case of the presence of several spatial structural forms of a biomolecule, it is not always clear how to distinguish between these forms for affiliation the characterized hydrogen atoms. Additional information can be obtained for the cases when kinetic measurements are carried out in conjunction with collision-induced dissociation of ions [9]. Alternative methods of ionization, e.g., MALDI, can be used for research not only on proteins and peptides but lipids as well [10].

Recently, an approach has been developed that allows performing on-line exchange reactions directly in the ion source with ionization by electrospray at atmospheric pressure [11–13]. The information obtained in these cases, as in many other works on the analysis of mass spectra of H/D exchange, is usually limited to the average number of exchanged hydrogen atoms for deuterium in the studied molecules. In some cases, when H/D exchange is carried out in the gas phase, it was shown that there are several structural conformations even within the same charge state of the protein and that these conformations can pass into each other [14]. Most often, such conclusions are made based on the observation of several local maxima in the intensity distributions of HDX fixed-charge ions. The transition from the folded to denatured form of the studied protein during HDX in the liquid phase by kinetic schemes EX1 or EX2 can also be established on this basis and peak width analysis [15]. The separation into Gaussian components of distributions of H/D substituted ions of a certain charge can also be used to characterize the transition between structural conformations of ions [10, 16].

For elucidation of structural information from distributions of related mass-spectral peaks, a new approach to analyze these data was developed and described in [17–22]. It is based on the decomposition of the mass spectra of biomolecules with a known primary structure, which in certain places undergo modification of the same type, for example, proton attachment or its release for certain groups in the molecule. Another possible type of related modification is demonstrated by the products of ion-molecular substitution reactions of certain atoms in the molecules, in particular, isotopic substitution in the HDX reaction. In all cases, when implementing the calculation scheme, the independence of the considered modifications in different localities for a specific structural form of the molecule was assumed. This assumption was confirmed by a number of decomposition calculations when initial data were approximated with applicable accuracy by distributions calculated through found probabilities of considered modifications for a given number of specific sites in the molecule. In all described examples,

the considered molecules had presumably a single preferable structural form. It was found that independent modifications result in a unimodal shape of calculated ion peak distribution (having a single local maximum). In all considered cases, this property was valid.

When characterizing the active centers of relatively simple molecules based on HDX reactions, the application of the proposed decomposition method to mass-spectral data provides quantitative information about a degree of activity of each of the H atoms, i.e., the probability of the HDX process for it [18]. This approach differs significantly from the simplified model for calculating the distributions of deuterium-substituted ions based on the division of exchanged hydrogen atoms into three sets, i.e., those quickly, intermediate, and slowly replaced by D atoms [16] with reaction rate constants that differ sequentially by an order of magnitude. The more detailed information obtained in our case can be useful to characterize the isomers in establishing the structure of the investigated sample. This knowledge is important in explaining the mechanism of the H/D exchange reactions.

All these data were processed in the context of the so-called one-dimensional decomposition procedure. A generalization of this approach to the case of an arbitrary number of charge carriers (multidimensional decomposition) was described and tested later [23–25]. In [26], we described an approach that combines the decomposition of two-dimensional mass and charge distributions with their separation into minimum number of components with found sets of probabilities for independent retention of charge carriers by ionogenic groups of a biomolecule. The results of testing this approach on two-dimensional mass–charge distributions of cytochrome *c* with H^+ and Na^+ as the charge carriers are also given there. In [27], we compared these results with a similar analysis of one-dimensional charge distributions for cytochrome *c* obtained by "convolution" of two-dimensional distributions and showed the importance of individual consideration of two charge carriers that form the biomolecule ions.

The next step was the development of the corresponding method for HDX in multicharged ions of biomolecules [28]. The main difference between this method and that described earlier [26] is taking into account a contribution of the natural isotopic distribution of the studied biomolecule to the observed distributions of HDX ions, which leads to their broadening. This requirement significantly reduces the applicability of the method. To calculate the natural isotopic distribution of this molecule, its elemental composition should be known.

In fact, the exact natural isotopic distribution of the analyzed biomolecule may not be known. For such cases, a method suitable for such situations should be developed. The aim of the present work is expanding the possibilities of the previous approach without using the "exact" natural isotopic distribution included in the observed H/D distributions. Another objective is determining the conditions for the adequacy of analysis of H/D exchange data on this basis for biomolecules and their complexes.

Materials/methods

The apamin HDX mass spectra obtained earlier [28] were used as initial data to test the proposed approach for analysis of HDX electrospray mass spectra in the case of an unknown natural isotopic distribution of biomolecules. These mass spectra are shown in Fig. 1 by the insertions A (1–3), B (1–3), and C (1–3).

The mass spectra were acquired using a high-resolution time-of-flight mass spectrometer with orthogonal ion injection (Ortho-TOFMS) [29]. A segmented radio-frequency quadrupole operating in continuous ion transfer mode was used as a molecular-ion reactor. To obtain the apamin ions, an apamin solution at a concentration of 10 μM in a mixture with CH_3OH, H_2O, and HCOOH at a volume ratio of the components $V_{H2O}:V_{CH3OH}:V_{HCOOH} = 100:400:1$ with pH = 3.16 was fed into the electrospray ion source. Three apamin mass spectra for the ions with charges from $z = 2$ to $z = 4$ were used for calculations under different conditions of the ND_3 feed into the reactor: Fig. 1A, without ND_3 feed; Fig. 1B, under continuous flow of ND_3 in a mixture with N_2 at the N_2:ND_3component ratio of 9:1, concentration of ND_3 molecules in the reaction zone being of ~ 10^{14} cm^{-3}; Fig. 1C, after turning off the flow of ND_3 molecules, a residual air pressure in the reactor being ~ 20 mTorr. In addition to the peaks of the apamin ions, the mass spectra included the corresponding peaks shifted along the mass scale by about 560 Da (Fig. 1D–F). It means that probably mass spectra of the apamin complex with some adducts were found. These mass spectra also contain peaks corresponding to 5-charged ions of a complex of an apamin molecule with some adduct. Estimations of the ion m/z values corresponding to some peaks are shown near the arrows of the lines coming from the tops of these peaks. They are calculated as centroids of these peaks cut off at their half heights. Mass values corresponding to some monoisotopic peaks are calculated from their found m/z values. The masses marked by red correspond to their elemental compositions. Shifts in the mass of small peaks related to the largest peaks in HDX distributions are marked by red as well.

To provide more exact confirmation of measured mass spectra which belong to apamin with elemental composition C79H131N31O24S4 and monoisotopic mass 2025.886 Da, two types of mass scale calibration of time-of-flight mass spectra were used. One of them uses two mass-spectral peaks of compounds specially added to the investigated solution. Such calibration was used in mass spectrum recorded before introducing the gas flow with ND_3. This mass spectrum is

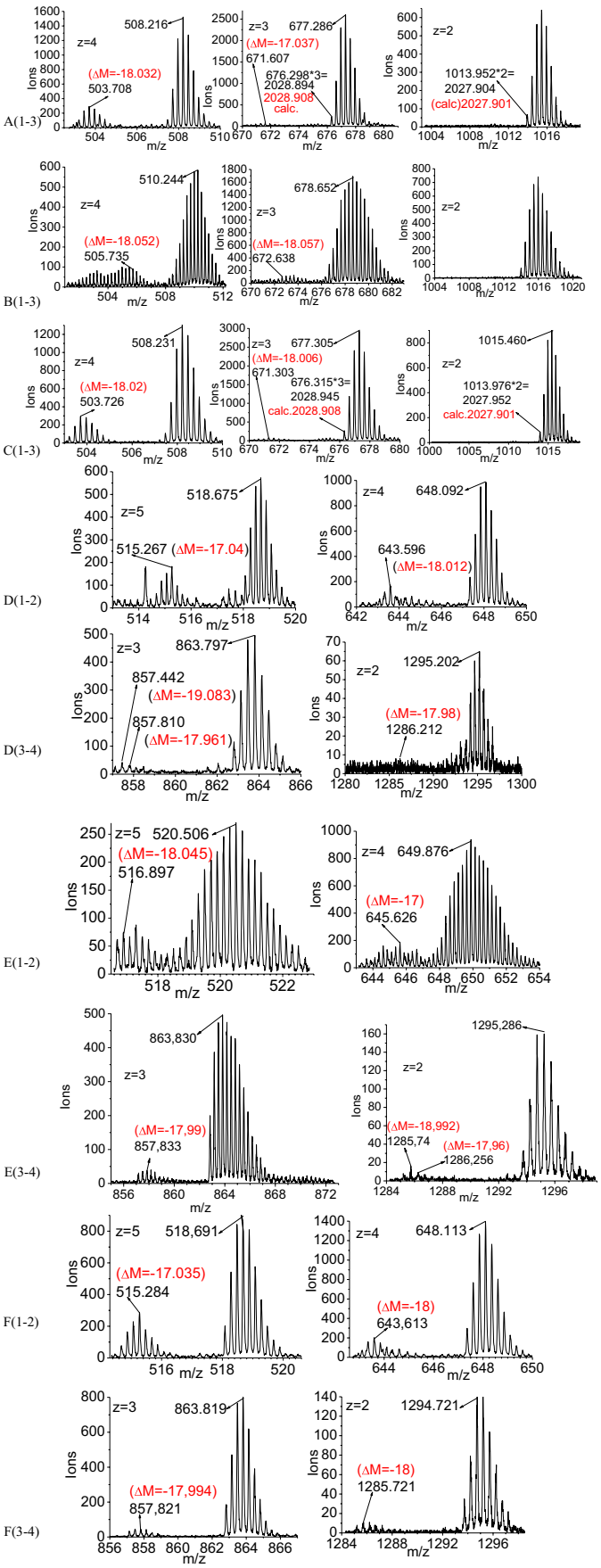

Fig. 1 The mass spectra of multicharged HDX apamin ions: **A** no ND_3 feed into the reactor (ApaIni), **B** the gas flow with ND_3 was introduced into the reactor ($ApaND_3$), **C** the gas flow was turned off (ApaF), **D**–**F** the corresponding mass spectra of apamin complex ions in the same order of changes in the mass spectra acquisition conditions as for **A**–**C**

presented in insertion A (1–3) of Fig. 1. Another approach uses large-enough peaks in HDX distributions of apamin itself for calibration of the mass scale in the considered mass spectrum. It was performed for the mass spectrum given in insertion C (1–3). The latter approach is less convenient as the shifts caused by an influence of natural isotopic peaks should be taken into account. However, the precision of such calibration may be better. Acceptable confirmation of the expected apamin composition was obtained for both types of calibration. A comparison of the measured and calculated masses (marked by red) for the first peaks in HDX distributions is given in graphs A (2, 3) and C (2, 3). Also, the increased probability to form a "circular" structure of apamin ions as the ion charge increases by connecting, for example, their C- and N-terminuses was confirmed by losing the water molecule whose mass is close to 18 Da. The corresponding mass loss is marked by red in graphs A1, B1, B2, C1, C3, D2, D3, D4, E1, E3, E4, F2, F3, and F4. Visible loss of 17 Da in A2, D1, E2, and F1 may correspond to additional H/D exchange of the produced amide H-atom after coming out of H_2O and connecting, for example, the C- and N-terminuses. Mass difference close to 19 Da may be explained by a loss of deuterated water molecule HDO. Practically, no such events were observed for two-charge ions (graphs A3, B3, and C3). It probably means that in two-charge ions, charge carriers are strongly connected with side chains of arginine residues in apamin, and even one of them cannot transfer to the N-terminus of apamin to attract the possibly negative C-terminus to form an amide bond and to lose a water molecule. It is interesting to note that noticeable ion peaks corresponding to the loss of a water molecule were found for double-charged peaks of apamin complex ions: D4, E4, and F4. It may correspond to the connection of the adduct to the apamin molecule by some transformation of at least one arginine residue in the apamin molecule, which can significantly reduce its affinity to H^+ and D^+ ions. Another possibility to lose the water is producing this molecule by the adduct itself. For example, in case this adduct is some small peptide, its N-terminus may become connected to the corresponding C-terminus with loss of the water molecule.

Differences in the m/z of the corresponding intense ions in the mass spectra of apamin and the apamin complex give estimates of the adduct mass, since the shifts of their measured m/z values caused by overlap of natural isotopes do not exceed 0.001 Da. Estimation of the adduct mass for 4- and 3-charged ions in mass spectra (D, A) are $(648.092 - 508.216) \times 4 = 559.504$ Da and $(863.797 - 677.286) \times 3 = 559.533$ Da. The same estimations for 4-charged corresponding ions in mass spectra (F2, C1) is $(648.113 - 508.231) \times 4 = 559.528$ Da. Such estimations for 3- and 2-charged ions mass spectra (F, C) are $(863.819 - 677.305) \times 3 = 559.542$ Da and $(1294.721 - 1015.46) \times 2 = 558.522$ $(+1.006 = 559.528)$ Da. The last maximal peak for $z = 2$ of the apamin complex is shifted down the mass scale by one H/D exchange with mass difference ~ 1.006 Da. The average value of adduct mass estimations is 559.527 Da. So the expected monoisotopic mass of the apamin complex is $2025.886 + 559.527 = 2585.413$ Da.

The main assumption for the development of our approach for HDX analysis is proposed mutual independence of HDX processes and charge retention processes for each structural form of a biomolecule. The independence of the charge retention was mainly demonstrated earlier [17, 21, 22]. Since H/D exchange for some labile H atom leads to minimal change in the ion mass, such modification has preferable chances compared to other modifications (e.g., attachment of alkali ions instead of H^+) to have no noticeable influence for HDX for other labile H atoms of the ion. Our recent measurements for HDX in NH_3^+ and H_2O^+ ions show the applicability of binomial distributions valid for independent equally probable HDX despite the fact that all exchangeable H atoms in these ions are located close to each other [30]. Another example of HDX of 23 equivalent H atoms in the negative ion cluster of 8 molecules H_3PO_4 shows that binomial distribution is also valid in this case [12]. The only known reason to produce some deviation from such independence may be HDX for H atoms participating in hydrogen bonds. Here, the changes in molecule structure are expected because HDX in this case is possible mainly when the corresponding hydrogen bond is destroyed by some molecule fluctuation [31]. The probability of such event is rather small, so enumeration of number HDX events in globular proteins of known primary structure may give estimation of H atoms producing hydrogen bonds in these proteins in solutions [32]. The independence of HDX from the ion charge for a given ion structure was confirmed by relevant measurements [33].

Actually, HDX for multi-charged biomolecule ions is similar to replacements of protons by other charge carriers, for example, sodium ions [27]. Such substitutions are equivalent to H^+, Na^+, or D^+ possible attachment to some specific sites of a formed virtual negative ion. These sites of the virtual ion are considered to be formally or actually deprotonated. In case of HDX for peptides and proteins, such residues may comprise besides acidic protons (a) amide H atoms adjacent to peptide bonds with exception of proline residue and (b) H atoms linked to N, O, and S atoms in the side chains of amino acid residues. Basic amino acid residues, including N-terminal amino acid, are considered to be not protonated in the virtual ion. The main feature in this situation is that the natural isotope distribution of the atoms included into the ion is superimposed on the mass spectra of H/D exchange and must be taken into account when analyzing these mass spectra. For other, heavier charge carriers (Na^+, K^+, and so on), natural isotopic distributions can usually be included into the composition of the convoluted ion peaks with known numbers of charge carriers of the considered mass and

charge distributions for corresponding data analysis. In [28], the formalism was developed to describe HDX in multiply charged ions. It may be considered as a special case of a mass and charge two-dimensional distribution.

The state of each biomolecule site with number i subjected to HDX may be described by a random variable δ_i with three outcomes: 1 (no charge carrier), H (a proton is attached), and D (a deuterium ion is retained). The charge sign $^+$ is omitted here for relative simplicity of the formalism description. For an ensemble of hypothetical biomolecule virtual ions with a single H/D substituting at the ith site, the expected distribution of the virtual ion with possible additional charge carriers can be described by the formal average value of the corresponding random variable δ_i, expressed as a corresponding trinomial:

$$E(\delta_i) = {}_0{}^iP + {}_H{}^iPH + {}_D{}^iPD$$

Here, ${}_0{}^iP$ is the probability for any charge carrier absence in the ith site, ${}_H{}^iP$ is the probability of proton retention for this site, and ${}_D{}^iP$ is the probability of the deuteron attachment at that location. H and D are considered as formal variables. Since these probabilities describe a complete set of incompatible events, their sum is equal to 1:

$${}_0{}^iP + {}_H{}^iP + {}_D{}^iP = 1$$

When the protons and deuterons are "attached" to N possible sites, an additional part Δ of the charge carrier composition of the virtual ion can be written as a product of random variables δ_i describing the states of the exchangeable sites of the biomolecule:

$$\Delta = \prod_{i=1}^{N} \delta_i$$

If the random variables δ_i are independent, then the average value of their product is equal to the product of the average values of these variables:

$$\begin{aligned} E(\Delta) &= E\left(\prod_{i=1}^{N} \delta_i\right) = \prod_{i=1}^{N} E(\delta_i) \\ &= \prod_{i=1}^{N} \left({}_0{}^iP + {}_H{}^iPH + {}_D{}^iPD\right) = \sum_{k,j=0}^{N} a_{kj} H^k D^j \end{aligned} \tag{1}$$

The resulting two-dimensional polynomial of the formal variables H and D describes the expected distribution of the ion peaks due to HDX at all possible N sites. At the same time, the term $a_{kj}H^kD^j$ corresponds to the peak of ions with k attached protons and j retained deuterons. The numerical value a_{kj} is equal to the relative intensity of this peak when normalized by the unit sum of these intensities:

$$\sum_{k,j=0}^{N} a_{kj} = 1$$

For comparison with the observed mass spectrum, it is necessary to take into account the natural isotopic distribution of the considered ions. To demonstrate the application of the developed method, apamin mass spectra obtained by electrospray of its solution were used. Apamin is a polypeptide consisting of 18 amino acids with a molecular monoisotopic mass of 2025.886 Da and elemental composition as it was pointed above:

$$C_{79}H_{131}N_{31}O_{24}S_4$$

Each of the atoms in this composition has a number of isotopes with known abundances and masses that are close in atomic mass scale to integer values.

Not taking into account the fine structure of isotopic peaks, which is only distinguishable for ultra-high-resolution mass spectrometers, such as ICR spectrometers and orbital ion traps, the polyisotopic composition of apamin leads to sequences of peaks similar to those of polyprotonated apamin with a step close to unit in the atomic mass scale. As upper estimation, there are 49 sites in apamin that are potentially capable of HDX [28], five of which may be positively charged. Since in this case 44 hydrogen atoms are assumed to be initially "removed" from the molecule, they will not participate in the "natural" isotopic distribution of the virtual apamin ion. So this isotopic distribution should be calculated for the composition $C_{79}H_{87}N_{31}O_{24}S_4$. The superposition of the "natural" isotopic distribution on the peaks of HDXions (1) leads to the splitting of these peaks with the shift of their masses and the conservation of charge. So the resulting observed HDX ion peak distribution should correspond to a polynomial written in the form (5) of [28]:

$$\begin{aligned} &\prod_{i=1}^{N} \left({}_0{}^iP + {}_H{}^iPH + {}_D{}^iPD\right) \\ &\cdot\left[0.2832 + 0.296\frac{D}{H} + 0.217\left(\frac{D}{H}\right)^2 + 0.1185\left(\frac{D}{H}\right)^3 + 0.0535\left(\frac{D}{H}\right)^4 + 0.0206\left(\frac{D}{H}\right)^5 + 0.0067\left(\frac{D}{H}\right)^6 + 0.0019\left(\frac{D}{H}\right)^7 + 0.0004\left(\frac{D}{H}\right)^8 + 0.0001\left(\frac{D}{H}\right)^9\right]. \end{aligned} \tag{2}$$

A set of the recorded peaks of multiply charged HDX ions for some biomolecule after normalization for unit sum of the areas of these peaks can be represented as a two-dimensional mass and charge distribution of ion intensities for the numbers of H^+ and D^+ held by this biomolecule virtual ion. It may be written as a power polynomial of two variables

of H and D in accordance with H^+ and D^+ with powers equal to the numbers of corresponding charge carriers and coefficients. The latters are equal to the areas of the corresponding peaks divided by the sum of the areas of all these peaks. Assuming the independence of H^+ or D^+retention by all sites, the observed H/D distribution for this structural apamin form should be approximated by the expression (2), where the values ${}_0{}^iP, {}_H{}^iP$, and ${}_D{}^iP$ must be determined. To do this, the corresponding decomposition procedure was developed without preliminary elimination of the "natural" isotopic distribution from the initial data [28].

Initially assuming a single structure form of the considered biomolecule, the values ${}_0{}^iP, {}_H{}^iP$, and${}_D{}^iP$ are searched iteratively when other values ${}_0{}^jP, {}_H{}^jP$, and${}_D{}^jP$ for $j \neq I$ in (2) are taken as they were previously found. The values ${}_0{}^iP, {}_H{}^iP$, and${}_D{}^iP$ under such conditions should minimize the squared deviation the distribution (2) from experimentally measured distribution of corresponding ion peak areas after their normalization to unit sum. Taking into account the essential property ${}_0{}^iP + {}_H{}^iP + {}_D{}^iP = 1$, the minimization procedure in this case is reduced to solving the linear system of two algebraic equations (with two variables, for example, ${}_H{}^iP$and${}_D{}^iP$) and taking also into account the following restrictions ${}_H{}^iP + {}_D{}^iP \leq 1, 0 \leq {}_H{}^iP \leq 1, 0 \leq {}_D{}^iP \leq 1$. After some number of these iterations when searched values remain the same with a given accuracy this step of searching procedure is considered to be finished.

In case the considered biomolecules are present in several space structural forms or conformations, it becomes impossible to approximate with expected accuracy the initial data on the base of the single polynomial (2). For this case, such approximation can be constructed as a linear combination of polynomials of the type (2) for a consistently increasing number of such forms with different sets of ${}_0{}^iP, {}_H{}^iP$, and${}_D{}^iP$. After that, the next level of iterations is organized. After establishing the first set of ${}_0{}^iP_1, {}_H{}^iP_1$,and${}_D{}^iP_1$, the corresponding HDX distribution calculated from this set with estimated the best factor of contribution is subtracted from initial data. The second set of ${}_0{}^iP_2, {}_H{}^iP_2$,and${}_D{}^iP_2$ is calculated for the found data difference by the same iteration procedure as described for the first set. After that the corresponding HDX distribution calculated from this second set with estimated the best factor of contribution is subtracted from initial data and this difference is used for recalculation of the first set. Further, the procedure is repeated with a new found the first set for searching the next approximation of the second set. This cycle of calculations is repeated for obtaining unchanging results for both sets of probability values with a given accuracy. In necessary cases iterative searching the next HDX component may be organized by subtracting the previous found components from initial data and returning to recalculation of the first component by subtracting all other found components from initial data and repeating the described iteration procedure. The calculations are finished in case the accuracy of initial data approximation by weighted sum of found HDX distributions is better than some expected value or contribution factor for some component becomes significantly negative. In the latter case, we return back to previous number of found components. In case this negative factor is rather small, the calculations may be continued and sometimes on the further steps of calculations this negative value may be replaced by some positive one.

In the original scale of conventional mass-spectrum recording (m/z), each of the found polynomials (2) is transformed into a set of unimodal distributions, the sum of which approximates the original data with acceptable accuracy [28]. This can be interpreted as a splitting the ensemble of observed biomolecule ions into its conformations without preliminary separating them and recording the corresponding individual mass spectra.

If the primary structure of the studied biomolecule is unknown its natural isotopic distribution cannot be calculated. There is one circumstance that allows us to hope to get rid of the need taking the natural isotopic distribution into account for separation of HDX mass spectra for sufficiently large biomolecules. The fixed-charge ion masses of a given biomolecule for independent HDX together with natural isotopic substitution of all other atoms can be considered as a sum of independent random variables with values equal to the possible mass for each atom of the biomolecule. Due to the statement of the central limit theorem of probability theory [34], for a sufficiently large number (N) of these random variables (with not zero or unit probabilities of atom isotopic substitution—significant independent random terms), the distribution of their sum may be approximated by some normal distribution (or Gaussian curve) with improving accuracy at increasing the N number. The normal distribution is characterized by only two parameters, i.e., the average or mean value and the variance. Therefore, with an increase of the number of significant independent random terms, the resulting distribution of their sum loses gradually some of its specific features. Accurate information about the terms number and their specific parameters that are invested in this resulting distribution is averagely converted to the values close to the average or mean value and variance of this distribution. In this case, we can expect that observed distribution under consideration can be approximated by "formal" HDX in a certain number of sites of the biomolecule without taking into account the natural isotopic distribution. And so found formal "probabilities" of charge carrier retention for a considered set of the biomolecule sites will have no former sense as in case of using natural isotopic distribution but their cumulate effect will result in distributions hopefully close to those received by the method realized in [28].

Results and discussion

The natural isotopic distributions of ions in the HDX mass spectra in our case can be represented as a sequence of relative areas with corresponding degrees of equivalent H/D substitutions in square brackets of formula (2). Replacing the influence of the natural isotopic distribution by corresponding change in HDX distribution, the initial data of a certain conformation of apamin or the apamin complex with the considered adduct can be approximated using the following product:

$$\prod_{i=1}^{N}\left({}_{0}{}^{i}\widetilde{P}+{}_{H}{}^{i}\widetilde{P}H+{}_{D}{}^{i}\widetilde{P}D\right) \quad (3)$$

The sign of tilde is used here to show that the searched values only formally play the role of probabilities of retention of charged carriers as in expression (2). Their function is to produce acceptable approximation of HDX distributions of components as it was occurred for expression (2).

Figure 2 shows the distributions of ion peak areas found from expressions (2) and (3) both in m/z scale and in HDX number scale, which are equivalent to integer shifts of isotope masses from the mass of the monoisotopic apamin ion. Figure 2A (1–3) presents three data sets in m/z scale from the mass spectra ApaF of 4-, 3-, and 2-charged apamin ions (Fig. 1C, 1–3). Contributions of four found sets of the apamin ions were calculated taking into account the natural isotopic distribution of the apamin molecule for 49 possible H^+ and D^+attachment sites in the molecule (N) and 5 potentially positively charged ones. Expression (2) with $N=49$ was used for that. The contributions are 92.2%, 3.9%, 3.5%, and 0.7%. The relative squared deviation of the sum of the four components from the initial spectral data (Σ^2) is 5.3. The values expressed in terms of Σ^2 are given to estimate the quality of the initial data approximation by the sum of the components. To obtain this estimate, before summing, the squared deviations are divided by the value of the initial data and after summing by the number of data points. Thus, in the case where the only error source is ion statistics, this value should be close to 1. A possible reason for the increase in this value is the contribution of chemical noise.

Figure 2B (1–4) presents the HDX distributions in HDX number scale of these four components for 2-, 3-, and 4-charged ions. The received data are approximated by Gaussian curves. Estimations of the average values and the widths of the corresponding Gaussian curves are presented as well. The errors of these values are close to each other for all ion charges, so they are shown only for the maximum Gaussian curve with ± before them.

Figure 2C (1–4) presents HDX distributions obtained by separating the same initial data, not taking into account the natural isotopic distribution of the apamin molecule based on expression (3) to approximate the searched data (ApaFnoIso).The presented results demonstrate a relatively good approximation of the found distributions by Gaussian curves and quite acceptable coincidence between the results obtained using both expressions (2) and (3). This means that for molecules with sizes of the apamin molecule and larger, it is quite acceptable to use expression (3) for the calculations without formally taking into account natural isotopic distributions. It is also interesting to note that HDX distributions for less ion charge comparing to that of increased by 1 ion charge are shifted in HDX scale to low values by the number not more than one. Such result is expected for the model of independent HDX reactions when additional H/D substitution may be prescribed to additional proton giving additional charge of the ion. Such property is valid almost for all found HDX distributions of apamin and apamin complex. Exceptions may be found for relatively small distributions and may be prescribed to enlarged errors of distributions localization in these cases.

Figure 2D and E present the results of data processing the residual HDX from the mass spectra (ApaIni) given in Fig. 1C. The number of possible H^+ and D^+attachment sites in the apamin molecule was 39, which is for 10 units less compared to the data on Fig. 2A–C. The values of the contributions of four found components are 91.8%, 3.7%, 4%, and 0.7%. Some difference for the main component with a contribution more than 90% can be explained by different concentrations of protonated water molecules in the reactor. During the electrospray process, water molecules penetrate into the mass spectrometer and provide a quasi-stationary concentration of H_3O^+ ions in the zone of residual HDX, probably on the surface of the interface at the entrance of the mass spectrometer. Apparently, the concentration of H_3O^+ ions in the reaction zone before turning on the flow with ND_3 is higher than after turning off the flow, since some of the H_3O^+ ions participate in HDX reactions. Attachment reactions of additional protons to 3-charged ions of apamin can be the reason for the relative increase in the peak intensity of 4-charged ions compared to the peak of 2-charged ions. Attachment of additional protons to ions of apamin inside the radio-frequency quadrupole is impossible as small ions such as H_3O^+ are discharged on quadrupole rods. The radio frequency and voltage applied to the quadrupole rods are selected so as to ensure high transmission of heavy ions and not to pass the light ions.

Figure 3 shows the results of separating the apamin mass spectra ApaND3 acquired in the case of the ND_3 introduction into the reactor (Fig. 1B). Two sets of conditions for this data processing were used. The first one is usual of the most previous calculations of apamin mass spectra. The number of exchangeable H atoms is 49 and the number of possible positively charged sites is 5. Figure 3A (1–3) presents three HDX distributions in m/z scale for the 4-, 3-, and 2-charged ions. Four components with contributions of

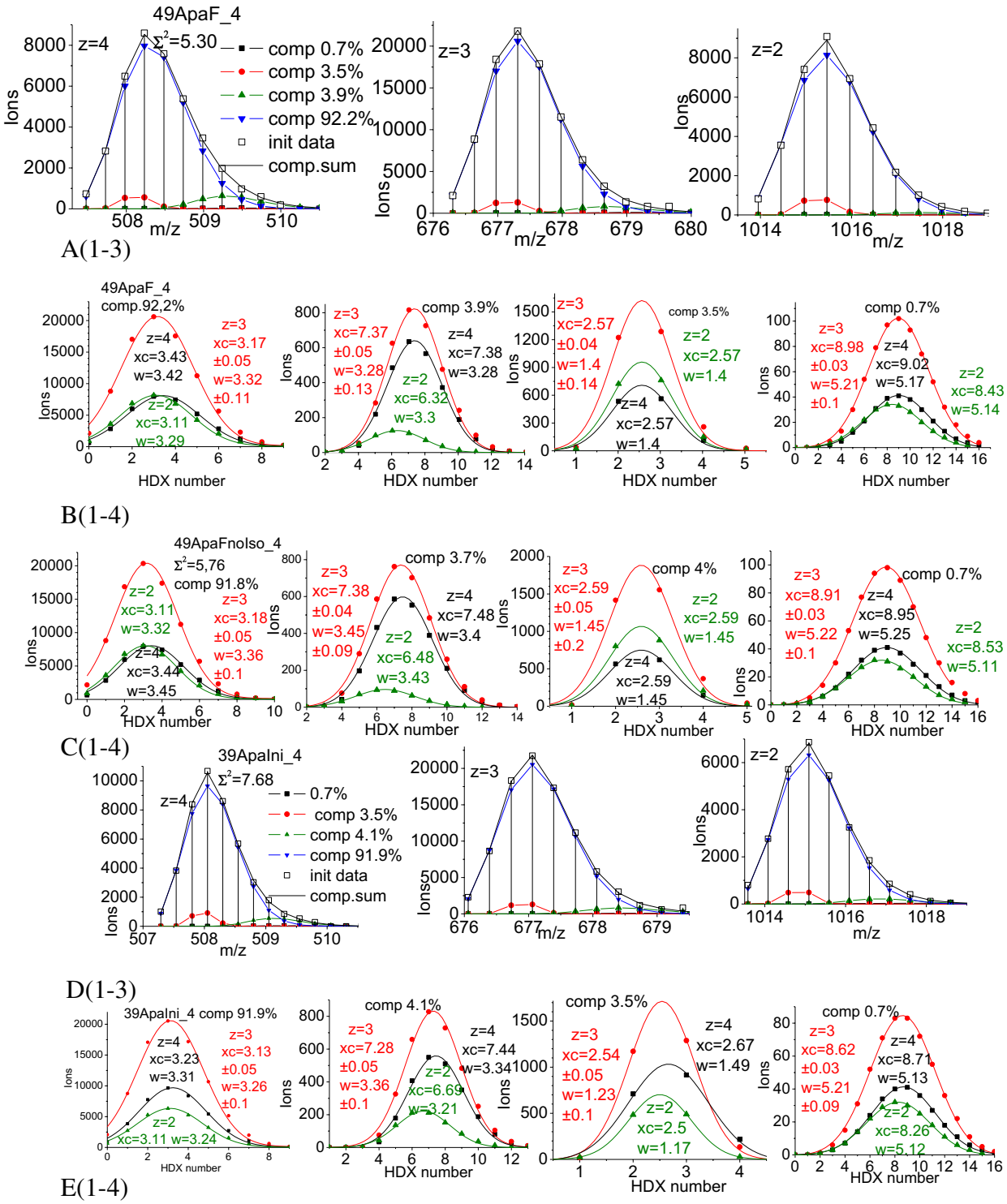

Fig. 2 The results of the separation of the apamin mass spectra acquired under conditions of no ND_3 introduction into the reactor (Fig. 1A, C): **A** the obtained peak areas and the sum of these areas in m/z scale for 4-, 3-, and 2-charged ions of four found components of the apamin ions from the mass spectra on Fig. 1A: white square—the obtained peak areas for 4-, 3-, and 2-charged ions; black solid line—the sum of four components; blue inverted triangle, green triangle, red circle, and black square—four components of the apamin ions with contributions of 92.2%, 3.9%, 3.5%, and 0.7%, respectively; **B** the HDX distributions in HDX number scale for four components after switching out the gas flow with ND_3: green triangle—2-charged ions; red circle—3-charged ions; black square—4-charged ions; green, red, and black lines—Gaussian curves approximating these data. The HDX distributions plots show the ion charges (z) and the positions of the Gaussian curves maxima (xc) and their width (w), which are twice the standard deviation of these curves; **C** the distributions by separating the same initial data without taking into account the natural isotopic distribution of the apamin molecule; **D**, **E** the corresponding separation results obtained for data from the mass spectra acquired before ND_3introduction into the reactor

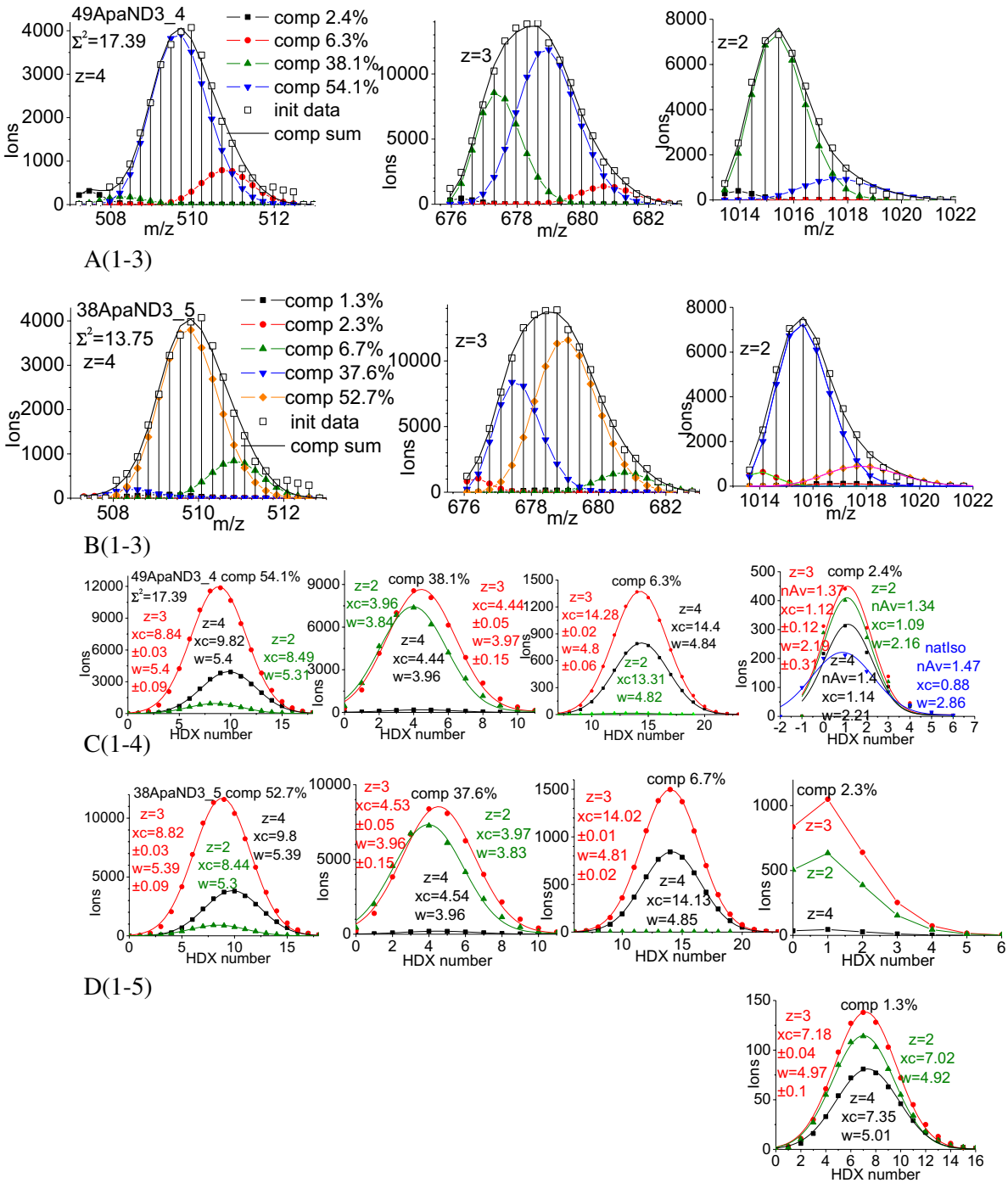

Fig. 3 The results of the separation of the apamin mass spectra acquired by introducing ND_3 into the reactor (Fig. 1B). **A** The results of searching components in the case of 49 H/D exchangeable sites and 4 potentially positively charged ones: white square—the obtained peak areas for 4-, 3-, and 2-charged ions; black line—the sum of four found components for the HDX distributions of the apamin ions in m/z scale; blue inverted triangle, green triangle, red circle, black square—four components with contributions of 54.1%, 38.1%, 6.3%, and 2.4%, respectively; **B** the results of searching components in the case of 38 H/D exchangeable sites and 4 potentially positively charged ones: white square—the obtained peak areas for 4-, 3-, and 2-charged ions; black line—the sum of five found components for the HDX distributions of the apamin ions in m/z scale; orange diamond, blue inverted triangle, green triangle, red circle, black square—five components with contributions of 52.7%, 37.6%, 6.7%, 2.3%, and 1.3%, respectively; **C** the HDX distributions in HDX numbers scale for the 2-, 3-, and 4-charged ions for four found components: green triangle—2-charged ions; red circle—3-charged ions; black square—4-charged ions; green, red, and black lines—Gaussian curves approximating these data. For comparison, data for the natural isotopic distribution (blue inverted triangle) are added to the plot of the component with contribution of 2.4%. The average value of the corresponding distribution was calculated in this case (nAv); **D** the HDX distributions for five found components: green triangle—2-charged ions; red circle—3-charged ions; black square—4-charged ions; green, red, and black Gaussian curves approximating these data. The data for the component with contribution of 2.3% are shown by broken lines

54.1%, 38.1%, 6.3%, and 2.4% were found in this case. As a result of attempts to distinguish additional components, the components with significant negative contributions were found. The relative squared deviation Σ^2 from the initial values for these data was found to be 17.39.

As two potential charge retention sites in apamin molecule are located very close to each other, namely the histidine side group at the N-terminus of the peptide and the NH_2 terminal group, it is reasonable to expect that these two sites can really work as a single charge location site. This can explain the absence of distinguishable peak of 5-charged ions in apamin mass spectra. Based on this assumption, one can likely reduce the number of possible charge locations to 4 and to repeat the search of apamin structural components for this case. It may be of additional interest to reduce the number of supposed H/D exchange sites, for example, to 38 as the calculation time becomes significantly shorter in this case. Figure 3B shows the results of the corresponding calculations. Five components with contributions of 52.7%, 37.6%, 6.7%, 2.3%, and 1.3% were found. The relative squared deviation of 13.75 was slightly less than that in previous case. Figure 3C (1–4) and D (1–5) presents the HDX distributions for 4 and 5 components, respectively. The distributions for the significant three components were found to be rather close to each other in both these cases. The components with contributions of 2.4% (Fig. 3C, 4) and 2.3% (Fig. 3D, 4) cannot be directly approximated with acceptable accuracy by Gaussian curves.

To provide Gaussian approximation of the data (Fig. 3C (4)) with 2.4% contribution, artificial zero data for virtual HDX number -1 was added to the real data.

Figure 4 shows the results of separating the data of the mass spectra of apamin complex ions (apamin molecule connected with an unknown adduct with a mass of about 560 Da) both before (Admixini) ND_3 introduction into the reactor and after (Admix) turning off the flow (Fig. 1, D to F).The number of potentially positive charged sites in this complex was accepted to be 6: 5 sites for the apamin molecule and 1 site for the adduct. The number of possible HDX sites in the absence of ND_3 introduction was taken to be 30, and the number of such sites under conditions after the flow was turned off was assumed to be 50. The relative squared deviations were 4.25 and 5.22 for the first and the second cases, respectively. In the first case, five components were found with contributions of 87.8%, 8.4%, 3.2%, 0.7%, and 0.1%. In the second case, four components were determined with contributions of 90.5%, 7.5%, 3%, and 0.04%. The HDX distributions shown in m/z scale look very similar in both cases. The shapes of the HDX distributions in HDX numbers scale for the main components are similar in both cases (Fig. 4B, 1, 2; D, 1, 2); moreover, they are similar to the HDX distribution shapes for the main components of the apamin ions (Fig. 2B, 1, 2; C, 1, 2; E, 1, 2). However, the mean values of the HDX distributions for apamin complex ions unexpectedly turned out to be less than those for the apamin ions by about 0.3–1.1. Perhaps, this means that the formation of the apamin complex occurs in the liquid phase in the electrospray ion source, and the connection between the apamin molecule and the adduct may be provided by an H-bond formation. As the H atom involved in H-bonds has a lower probability of H/D exchange, positions of HDX distributions can shift to the left. The components with contributions of 3.2% (Fig. 4B, 5) and 3% (Fig. 4D, 3) cannot be directly approximated with acceptable accuracy by Gaussian curves.

Figure 5 shows the results of separating the mass spectra of the apamin complex ions acquired under conditions of the ND_3 introduction into the reactor (Fig. 1E). These results were obtained for different numbers of possible HDX sites and different numbers of potentially charged sites. In cases with 49 (5 potentially charged sites) and 50 possible HDX sites (6 potentially charged sites), seven components were found (Fig. 5A–D, 1–2). The values of the relative squared deviations from the original data were 13.36 and 10.74, respectively. In the case of 30 possible HDX sites (6 potentially charged sites), ten components were found (maximum possible number for our computer program) with one small negative component − 0.6% (Figs. 5, A–D; 3). The value of the relative squared deviation Σ^2 in this case is 5.61. It means that the proposed model for approximating the obtained HDX data by components with independent HDX events for some number of sites can also be considered as valid in the case of the apamin complex.

Conclusions

The previously developed method [28] for the decomposition and the separation of HDX mass spectra of multiply charged ions of biomolecules with known natural isotope distributions was modified for use in the case of unknown natural isotope distributions of the biomolecules. This method was tested on the same apamin mass spectra as in [28], and on mass spectra of a complex of apamin molecule with unknown adduct with molecular mass of about 560 Da. The results of separating the apamin mass spectra without taking into account the natural isotopic distribution of apamin molecule turned out to be almost identical to those presented in [28]. The errors in estimating the distributions of the components and their contributions were no more than 2–3% of the maximum values. It is probably due to the action of the central limit theorem, when the observed HDX distributions can be approximated with increasing accuracy by normal distributions with an increase in the number of substituted H atoms for independent H–D substitution of labile hydrogen atoms. Therefore, it is possible to conclude that the developed approach to the analysis of HDX distributions of multiply charged ions without taking into account their natural isotope distributions will be quite adequate for sufficiently large biomolecules with

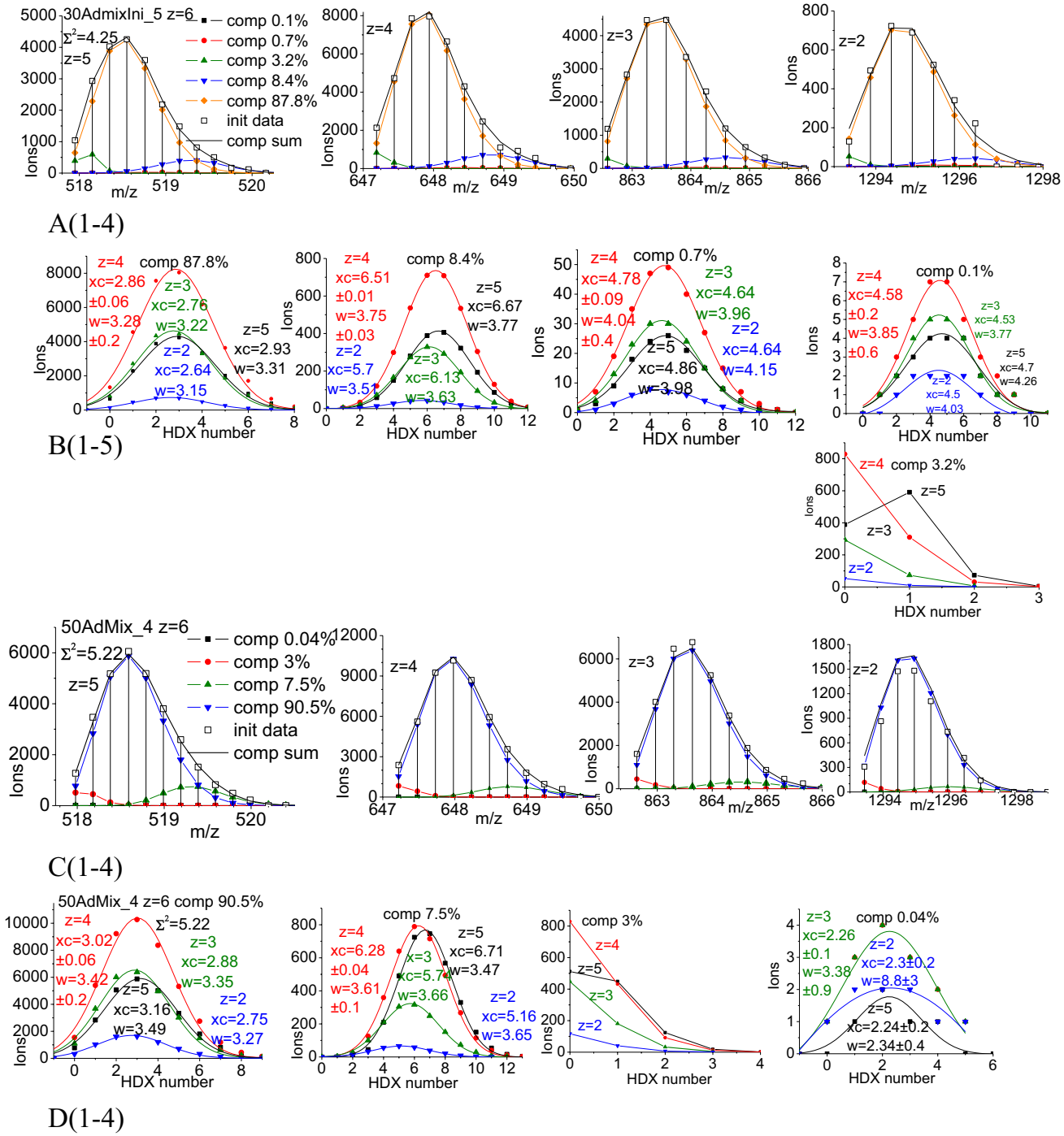

Fig. 4 The results of the separation of the apamin complex ion mass spectra acquired under conditions of no ND_3 introduction into the reactor (Fig. 1D, F). **A**—the results of searching components in the case of 30 possible HDX sites and 6 potentially positively charged ones: white square—the obtained peak areas for 5-, 4-, 3-, and 2-charged ions; black line—the sum of five found components; orange diamond, blue inverted triangle, green triangle, red circle, black square—five components of the apamin complex ions with contributions of 87.8%, 8.4%, 3.2%, 0.7%, and 0.1%, respectively; **B** the HDX distributions in HDX numbers scale for the 2-, 3-, 4-, and 5-charged ions for five components: blue inverted triange—2-charged ions; green triangle—3-charged ions; red circle—4-charged ions; black square—5-charged ions; blue, green, and red lines and black line—Gaussian curves approximating these data. The data for the component with contribution of 3.2% are shown by broken lines; **C** the results of searching components in the case of 50 possible HDX sites and 6 potentially positively charged ones: white square—the obtained peak areas for 5-, 4-, 3-, and 2-charged ions; black line—the sum of four found components; blue inverted triangle, green triangle, red circle, black square—four components of the apamin complex ions with contributions of 90.5%, 7.5%, 3%, and 0.04%, respectively; **D** the HDX distributions for four components: blue inverted triangle—2-charged ions; green triangle—3-charged ions; red circle—4-charged ions; black square—5-charged ions; blue, green, red, and black line—Gaussian curves approximating these data. The data for the component with contribution of 3% are shown by broken lines

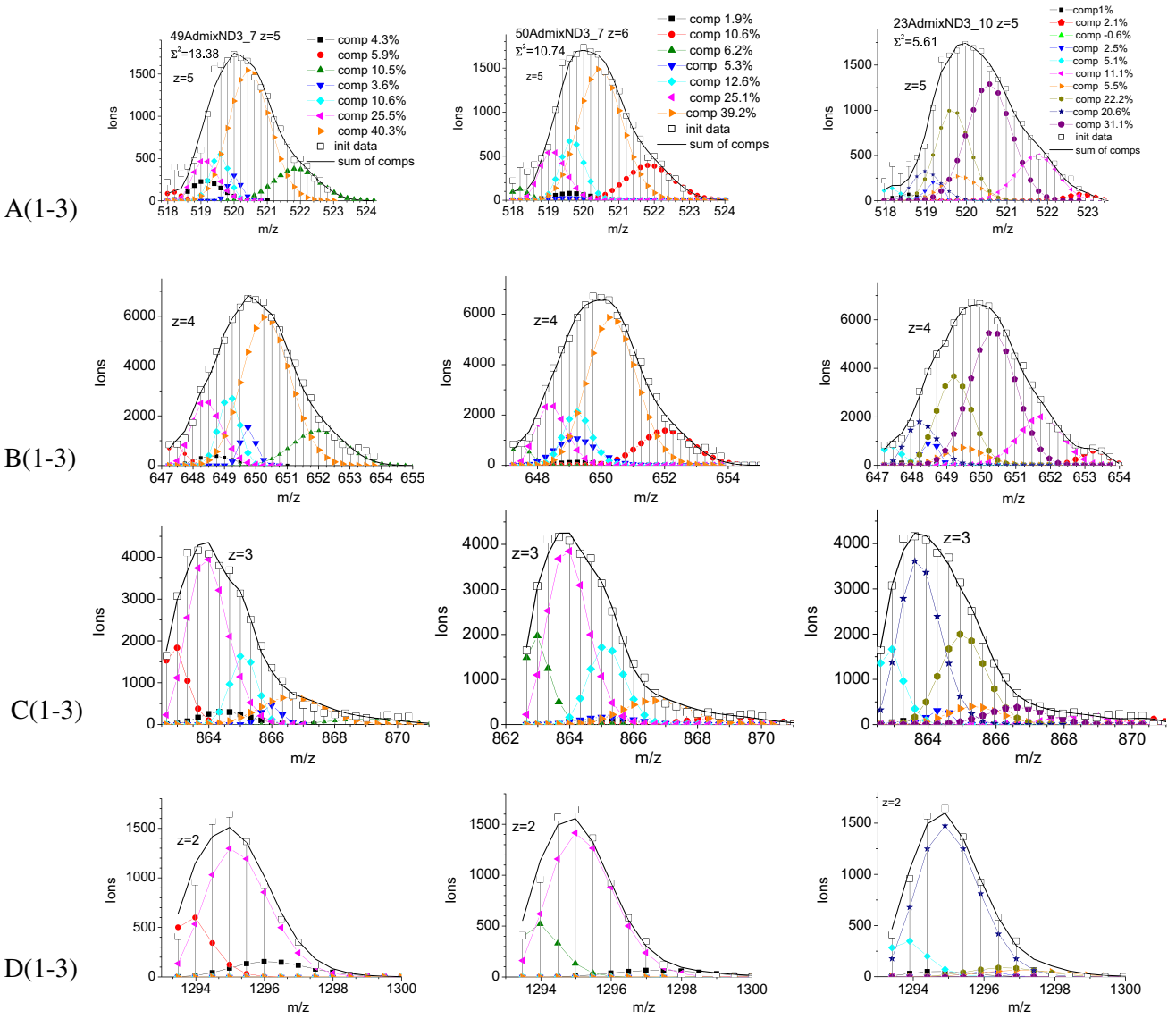

Fig. 5 The results of the separation for the mass spectra of the apamin complex ions acquired by introducing ND_3 into the reactor (Fig. 1E). **A**–**D** (1)—the results of searching components in the case of 49 H/D exchangeable sites and 5 potentially positively charged ones: white square—the obtained peak areas for 5-, 4-, 3-, and 2-charged ions; black line—the sum of seven found components; orange triangle,…, black square—the seven components with contributions of 40.3%, …, and 4.3%, respectively; **A**–**D** (2)—the results of searching components in the case of 50 H/D exchangeable sites and 6 potentially positively charged ones: white square—the obtained peak areas for 5-, 4-, 3-, and 2-charged ions; black line—the sum of seven found components; orange triangle,…, black square—the seven components with contributions of 39.2%,…, and 1.9%, respectively; **A**–**D** (3)—the results of searching components in the case of 30 H/D exchangeable sites and 6 potentially positively charged ones: white square—the obtained peak areas for 5-, 4-, 3-, and 2-charged ions; black line—the sum of ten found components; violet circle, …, black square—the ten components with contributions of 31.1%, …, and 1.0%, respectively

an increase in accuracy for larger molecules. The Gaussian approximation used for the observed HDX distributions of the apamin ions proved to be quite acceptable. Only small deviations from the initial data can be observed in the "tails" of the Gaussian curves. An even better approximation can be seen for the apamin complex being about 25% heavier than the apamin molecule. Calculations performed for a reduced number of H/D exchangeable sites and a reduced number of ones able to retain charge carriers gave similar results of the HDX distribution separation. Thus, exact information about the numbers of such sites may not be needed to obtain acceptable information about composition of observed HDX distribution, and our assumption of independence HDX processes seems to be correct.

The numbers of the found main components (3) are the same for the apamin molecule and the apamin complex in the case of ND_3 introduction into the reactor, and the calculated contributions are rather close. Probably, it indicates that the structural

conformation of the apamin complex is close to that for the apamin molecule. This is confirmed by the fact that the shifts in the positions of the H/D distributions for the two largest components of the complex in HDX number scale relative to those for apamin molecule are practically the same.

The obtained data for residual H/D distribution maxima mass shifts for adduct attachment being less than average molecular mass of adduct may be explained by attachment of adduct in the liquid phase before H/D exchange. Adduct attachment to apamin molecule after HDX should result to mass shift less than mass of adduct. Probably, it means that the adduct is present in the initial apamin solution used in the measurements.

Insufficient resolution of initial data may be the reason for the developed method to be prevented for application at increase of biomolecule sizes. One outlet here is transition to other ways of isotopic exchange, for example, $O^{16}$for O^{18} [35]. Another way is recorded ion charge reducing [36]. Essential step for mass spectra analysis of large molecules may be direct approximation of received isotopic distributions by Gaussian curves, as such approximation should become more and more applicable with increase of biomolecule sizes due to central limit theorem [34].

Acknowledgements We thank Dr.Sci. Tatyanenko L.V. and PhD Raznikov A.V. for helpful discussions of some topics connected with this paper.

Funding This work was performed in accordance with the state tasks, state registration №: 122040500059-8 and № AAAA-A19-119022690098–3.

Declarations

Conflict of interest The authors declare no competing interests.

References

1. Kaltashov IA, Eyles SJ. Studies of biomolecular conformations and conformational dynamics by mass spectrometry. Mass Spectrom Rev. 2002;21:37–71.
2. Masson GR, Burke JE, Ahn NG, et.al. 2019 Recommendations for performing, interpreting and reporting hydrogen deuterium exchange mass spectrometry HDX-MS experiments Nature Methods 596 595–602
3. Zhang Z, Smith DL. Determination of amide hydrogen exchange by mass spectrometry: a new tool for protein structure elucidation. Protein Sci. 1993;2:522–31.
4. Kostyukevich Y, Acter T, Zherebker A, Ahmed A, Kim S, Nikolaev E. Hydrogen deuterium exchange in mass spectrometry. Mass Spec Rev. 2018;1:43. https://doi.org/10.1002/mas.21565.
5. Deng B, Lento C. Wilson DJ Hydrogen deuterium exchange mass spectrometry in biopharmaceutical discovery and development - a review. Anal Chim Acta. 2016;940:8–20. https://doi.org/10.1016/j.aca.2016.08.006.
6. Abzalimov RR, Kaltashov IA. Controlling hydrogen scrambling in multiply charged protein ions during collisional activation: implications for top-down hydrogen/deuterium exchange MS utilizing collisional activation in the gas phase. Anal Chem. 2010;82:942–50.
7. Green MK, Lebrilla CB. Ion-molecule reactions as probes of gas-phase structures of peptides and proteins. Mass Spectrom Rev. 1997;16:53–71.
8. Robinson EW, Williams ER. Multidimensional separations of ubiquitin conformers in the gas phase: relating ion cross sections to H/D exchange measurements. J Am Soc Mass Spectrom. 2005;16:1427–37. https://doi.org/10.1016/j.jasms.2005.04.007.
9. Xiao H, Hoerner JK, Eyles SJ, Dobo A, Voigtman E, Melcuk AI, et al. Mapping protein energy landscapes with amide hydrogen exchange and mass spectrometry I a generalized model for a two-state protein and comparison with experiment. Protein Sci. 2005;14(543):57.
10. Abzalimov RR, Kaltashov IA. Extraction of local hydrogen exchange data from HDX CAD MS measurements by deconvolution of isotopic distributions of fragment ions. J Am Soc Mass spectrom. 2006;17:1543–51. https://doi.org/10.1016/j.jasms.2006.07.017.
11. Kostyukevich Y, Gleb Vladimirov, Stekolschikova E, Ivanov D, Yablokov A, Zherebker A, Sosnin S, Orlov A, Fedorov M, Khaitovich P and Nikolaev E. 2019 Hydrogen deuterium exchange aiding compound identification for LC MS and MALDI imaging lipidomics Anal Chem 91 13465 74
12. Kostyukevich Y, Kononikhin A, Popov I, Nikolaev E. Simple atmospheric hydrogen/deuterium exchange method for enumeration of labile hydrogens by electrospray ionization mass spectrometry. Anal Chem. 2013;85:5330–4.
13. Kostyukevich Y, Kononikhin A, Popov I, et al. Enumeration of labile hydrogens in natural organic matter by use of hydrogen/deuterium exchange Fourier transform ion cyclotron resonance mass spectrometry. Anal Chem. 2013;85:11007–13.
14. Kostyukevich Y, Kononikhin A, Popov I, Spasskiy A, Nikolaev E. In ESI-source H/D exchange under atmospheric pressure for peptides and proteins of different molecular weights from 1 to 66 kDa: the role of the temperature of the desolvating capillary on H/D exchange. J Mass Spectrom. 2015;50:49–55.
15. Valentine SJ, Clemmer DE. H/D exchange levels of shape-resolved cytochrome c conformers in the gas phase. J Am Chem Soc. 1997;119:3558–66.
16. Weis DD, Wales TE, Engen JR. Hotchko M and Eyck LFT Identification and characterization of EX1 kinetics in H/D exchange mass spectrometry by peak width analysis. J Am Soc Mass Spectrom. 2006;17:1498–509. https://doi.org/10.1016/j.jasms.2006.05.014.
17. Raznikova MO, Raznikov VV. Evaluating the probability of protonation of amino acids in peptides and proteins according to their electrospray mass spectra. Khim Fiz. 2001;20:13–7.
18. Raznikova MO, Raznikov VV. Determination of the activity of H atoms of ions of polyfunctional compounds on the basis of mass spectra of H/D exchange. Journal of Advances in Chemical Physics. 2005;4:16–22.
19. Raznikova MO, Raznikov VV. A new approach to the analysis of the kinetics of H/D exchange processes of active hydrogen atoms of polyfunctional compounds. Mass-spectrometrija. 2006;3:193–200.
20. Raznikov VV, Raznikova MO. 2009 Decomposition of charge-state distributions for better understanding of electrospray mass spectra of bioorganic compounds Part 1 Basic formalism Eur J Mass Spectrom 15 367 75 https://doi.org/10.1255/ejms.994
21. Raznikov VV, Raznikova MO. 2009 Decomposition of charge-state distributions for better understanding of electrospray mass spectra of bioorganic compounds Part 2 Application of the method Eur J Mass Spectrom 15 377 83 https://doi.org/10.1255/ejms.995.
22. Raznikov VV, Raznikova MO. Use of decomposition of ion charge-state distributions for the interpretation of electrospray ionization mass spectra of bioorganic compounds. J Anal Chem.

2012;67:974–80. https://doi.org/10.1134/s1061934812130084. Translated from Mass-spectrometrija. 2011;8:181–8.
23. Raznikov VV, Raznikova MO. 2014 Decomposition of multidimensional charge-state distributions of ions produced by electrospray ionization of bioorganic compounds. Part 1 Basic formalism and implementation of the method. J Anal Chem 69 1270–7 https://doi.org/10.1134/S1061934814130073. Translated from Mass-spectrometrija 2013 10 175 182
24. Raznikov VV, Raznikova MO. 2014 Decomposition of multidimensional charge-state distributions of ions produced by electrospray ionization of bioorganic compounds Part 2 Testing of the method for one-dimensional distributions J Anal Chem 69 1278–84 https://doi.org/10.1134/S1061934814130085. Translated from Mass-spectrometrija. 2013;10:183–9.
25. Raznikov VV, Raznikova MO, Pridatchenko ML. Disentangling of information about the structure of biomolecules based on the decomposition and separation of two-dimentional charge distributions of ions. J Anal Chem. 2017;72:1300–6. https://doi.org/10.1134/S106193481713007X. Translated from Mass-spectrometrija. 2016;13:124–31.
26. Raznikov VV, Raznikova MO. Characterization of the structural forms of biomolecules based on the decomposition and separation of the charge state distributions of their ions. J Anal Chem. 2019;74:1277–85. https://doi.org/10.1134/S1061934819130112. Translated from Mass-spectrometrija. 2018;15:152–61.
27. Raznikova MO, Raznikov VV. Calculation of the characteristics of the ionic states of cytochrome *c* biomolecules by a decomposition method with separation of one- and two-dimensional ion charge distributions. Russ J PhysChem B. 2018;12:271–80. https://doi.org/10.1134/S1990793118020252.
28. Raznikov VV, Raznikova MO, Sulimenkov IV. Two-dimensional decomposition of H-D exchange mass spectra of multicharged ions of biopolymers and their separation into components with independent H-D substitutions. Anal and Bioanal Chem. 2019;411:6409–17. https://doi.org/10.1007/s00216-019-02019-2.
29 Dodonov AF, Kozlovski VI, Soulimenkov IV, Raznikov VV, Loboda AV, Zhen Zhou, Horwath T, Wollnik H. High-resolution electrospray ionization orthogonal-injection time-of-flight mass spectrometer // *Eur*. J Mass Spectrom. 2000;6(6):481–90.
30. Raznikov VV, Zelenov VV, Aparina EV, Sulimenkov IV, Raznikova MO. 2020 Formation of deuterium-substituted ions from a solution introduced into a radio-frequency quadrupole under the action of a gas jet passed through an electron ionization ion source. Journal of Analytical Chemistry 2021 Vol 76 No 13 pp 1–8 Russian Text © The Author(s) 2020 published in Mass-spektrometriya Vol 17 No 2 pp 103–111 https://doi.org/10.1134/S1061934821130116
31. Dempsey CE. PH dependence of hydrogen exchange from backbone peptide amides in apamin. Biochemistry. 1986;25:3904–11.
32. Suvorina MYu, Surin AK, Dovidchenko NV, Lobanov MYu, Galzitskaya OV. 2012 Comparison of experimental and theoretical data on hydrogen deuterium exchange for ten globular proteins Biochemistry Moscow 77 616 23
33. Wang F, Tang X. Conformational heterogeneity of stability of apomyoglobin studied by hydrogen/deuterium exchange and electrospray ionization mass spectrometry. Biochemistry. 1996;35:4069–78.
34. DasGupta A. Asymptotic theory of statistics and probability Springer 2008
35. Kostyukevich Y, Kononikhin A, Zherebker A, Popov I, Perminova I, Nikolaev E. Enumeration of non-labile oxygen atoms in dissolved organic matter by use of 16O/ 18O exchange and Fourier transform ion-cyclotron resonance mass spectrometry // *Anal*. Bioanal Chem. 2014;406(26):6655–64.
36. Yang Y., Ivanov D.G. and Kaltashov I.A. 2021 The challenge of structural heterogeneity in the native mass spectrometry studies of the SARS CoV 2 spike protein interactions with its host cell surface receptor //*Anal. Bioanal Chem* Vol 413 N29 P.7205–7214